

 Open access • Journal Article • DOI:10.1103/PHYSREVA.47.4114

Threshold and resonance phenomena in ultracold ground-state collisions

— [Source link](#) 

Eite Tiesinga, BJ Boudewijn Verhaar, H. T. C. Stoof

Institutions: Eindhoven University of Technology

Published on: 01 May 1993 - Physical Review A (American Physical Society)

Topics: Magnetic trap, Inelastic collision, Zeeman effect, Hyperfine structure and Ground state

Related papers:

- [Observation of Feshbach resonances in a Bose–Einstein condensate](#)
- [Observation of Bose-Einstein Condensation in a Dilute Atomic Vapor](#)
- [Observation of a Feshbach Resonance in Cold Atom Scattering](#)
- [Observation of Resonance Condensation of Fermionic Atom Pairs](#)
- [Bose-Einstein condensation in a gas of sodium atoms.](#)

Share this paper:    

View more about this paper here: <https://typeset.io/papers/threshold-and-resonance-phenomena-in-ultracold-ground-state-41dimaixms>

Threshold and resonance phenomena in ultracold ground-state collisions

E. Tiesinga, B. J. Verhaar, and H. T. C. Stoof

Department of Physics, Eindhoven University of Technology, 5600 MB Eindhoven, The Netherlands

(Received 8 October 1992)

We study the magnetic-field dependence of the cross sections for elastic and inelastic collisions of pairs of ultracold cesium atoms in a magnetic trap, calculated with the coupled-channels method. We pay special attention to atoms in the $f=3$, $m_f=-3$ weak-field seeking state of the lower hyperfine manifold. The cross sections show a pronounced resonance structure. We discuss its origin, starting from the pure bound singlet and triplet rovibrational Cs_2 states and introducing perturbations due to the hyperfine and Zeeman interactions. We also discuss the role of the centrifugal barrier in the final collision channel in reducing the loss of atoms from the trap due to transitions induced by the magnetic dipole-dipole interaction.

PACS number(s): 32.80.Pj, 06.30.Ft, 42.50.Vk

I. INTRODUCTION

Since the successful slowing down of a thermal atomic beam with the radiation pressure of a counterpropagating laser beam [1] in 1985, the ability to manipulate the position and velocity of atoms has increased tremendously. A variety of techniques has been developed to slow down atoms to Doppler and later to sub-Doppler velocities [2]. In addition, there has been rapid progress in developing techniques to trap cold atoms in magnetic, optical, and magneto-optic traps [2], and in doing experiments with freely falling atoms in an atomic fountain [3,4], and in an atomic trampoline [5], the latter being a trap in which the atoms are confined above by gravity and below by a concave mirror. All of these accomplishments are based on single-atom properties, i.e., the interaction of single atoms with external fields.

There is a growing awareness, however, of the importance of two-atom properties in all of these experimental circumstances. Contrary to ionic species with their strong Coulomb interaction, neutral atoms have the advantage that their number can be increased, for instance for improving the signal-to-noise ratio or for achieving the critical density for Bose condensation, without disastrous interparticle perturbations, leading to collisional frequency shifts or escape of atoms from traps. To find the admissible limits to densities which nevertheless exist, it is necessary to investigate hyperfine-state changing and nonchanging collisions. In two previous short papers we studied the role of such collisions in a cesium atomic fountain [6] and in a cesium magnetic trap [7].

The most spectacular envisaged application of the cesium fountain is the construction of an improved version of the cesium atomic clock with an estimated increase of accuracy by two orders of magnitude, made possible by the much longer time which slow atoms spend in a limited domain of space during their ballistic flight. Atoms are directed upward either with a pulse of light [5] or with "moving molasses" [4]. On their way up and down transitions between the ground-state hyperfine levels are induced by means of the Ramsey method of separated oscillatory fields. Owing to the slowness of the atoms the

time between the two microwave pulses used to induce the transition can be very long relative to that in the conventional cesium clock. In Ref. [6] we have shown that elastic collisions lead to frequency shifts with a profound influence on the accuracy and stability of the cesium fountain clock.

An intriguing aim of experiments with magnetically trapped cesium atoms is to observe quantum collective effects in a weakly interacting Bose gas, the so-called Bose-Einstein condensation (BEC). This occurs when the thermal de Broglie wavelength becomes comparable to the mean distance between the atoms or larger. In these circumstances it is favorable for the atoms to occupy the one-particle ground state macroscopically. The first such attempts dealt with atomic hydrogen. A gas sample of ground-state hydrogen atoms in the doubly polarized $(f, m_f)=(1, -1)$ hyperfine state was stored in a storage cell or gas bubble surrounded by superfluid ^4He down to temperatures of order 0.1 K. These attempts were hampered by an unacceptable limitation of the lifetime of the gas sample due to three-body recombination [8] at the high densities required for BEC. One way to avoid this difficulty is to use a relatively large buffer volume with lower densities to increase the lifetime of the total system. Another way is to store and evaporatively cool hydrogen atoms in a magnetic trap [9,10], which allows in principle the realization of BEC at much lower temperature-density combinations. Due to the impossibility of creating a static magnetic-field maximum in free space, only atoms in the weak-field-seeking doubly-polarized $(f, m_f)=(1, +1)$ state can be trapped. In this way temperatures of about 100 μK were reached [10]. Up to now none of these attempts have realized the ultimate goal of BEC.

The advent of laser cooling and manipulation techniques has created the perspective of realizing BEC in an ultracold gas of alkali-metal atoms. Suitable candidates on which experimental groups are concentrating are cesium [11] and lithium [12]. Optical and magneto-optic traps are unsuitable to realize the final stage of BEC: radiation pressure from light reemitted by trapped atoms limits the maximum atomic density [13]. A static mag-

netic trap in combination with evaporative cooling offers better prospects. Both atomic species have the important advantage relative to atomic hydrogen of a nuclear spin greater than $\frac{1}{2}$, so that their ground-state hyperfine diagram displays a weak-field-seeking state in the lower hyperfine manifold. As Wieman *et al.* pointed out [11], this offers the possibility to reduce the loss of atoms from exothermal collisions in which the interatomic magnetic-dipole force induces hyperfine transitions from s - to d -wave channels: for low magnetic-field strengths the atoms feel only the weak long-range part of the dipole force due to the centrifugal barrier in the final channel.

In Ref. [7] we discussed the prospects for achieving BEC in atomic cesium and found them to be promising especially if this $(f, m_f) = (3, -3)$ hyperfine level is used. BEC in a weakly interacting Bose gas such as cesium is only possible in the temporarily existing metastable state, in which hyperfine changing collisions or molecule formation in three-body collisions have not yet reduced the density of atoms in the original hyperfine state appreciably. Note that the situation for atomic hydrogen is in principle identical, the only difference being that the triplet H_2 system has no bound states, so that recombination can only occur via a spin flip induced by the dipolar force. In contrast, triplet Cs_2 has many bound states, so that recombination in a $Cs + Cs + Cs$ collision does not require spin flips. It follows from the foregoing that the realization of BEC is subject to severe conditions on the time scales of collision phenomena. The time scale for thermalizing elastic two-body collisions which are essential for evaporative cooling and for establishing the metastable state should be sufficiently short relative to the recombination time scale. In addition, for BEC to occur in the metastable state the two-body elastic collisions have to be effectively repulsive, i.e., a positive value for the scattering length is required in order for the condensed phase to be stable against collapse [14].

In this paper we will not repeat the line of reasoning and the results of Ref. [7] with respect to these conditions. Instead, this paper will be devoted to a more extensive presentation of some aspects of the work which have received insufficient attention in our previous short papers [6,7], notably the pronounced Feshbach-type resonance structure in the magnetic-field dependence of the theoretical elastic and inelastic two-body relaxation rates predicted by our calculations and the role of the final centrifugal barrier in reducing the loss of atoms. A related resonance structure has previously been predicted [15] for more general diatomic systems and observed [16,17] for gas samples of atomic hydrogen: the inverse-predissociation phenomenon. In this paper we show that it also occurs in dipolar transitions and at weak fields.

The paper is organized as follows. In Sec. II we discuss in some detail the two-body theory needed. Extensive attention will be given to the symmetry aspects of the various interaction terms as desired for the understanding of resonances in elastic and exchange scattering in Sec. III and in dipolar scattering in Sec. IV. In Sec. V we will go into the role of the centrifugal barrier in the final channel in determining the behavior of the dipolar rates. Some conclusions are finally given in Sec. VI.

II. INTERACTION TERMS, SYMMETRIES, AND METHOD OF CALCULATION

We consider the collision of two ground-state cesium atoms in a (local) magnetic field along the z axis. We start from the effective two-body Hamiltonian [7,18]

$$H = \frac{\mathbf{p}^2}{2\mu} + \sum_{i=1}^2 (V_i^{\text{hf}} + V_i^Z) + V^c + V^d, \quad (1)$$

comprising a kinetic-energy term with μ the reduced mass, single-atom hyperfine and Zeeman terms

$$V^{\text{hf}} = \frac{a_{\text{hf}}}{\hbar^2} \mathbf{S}^e \cdot \mathbf{S}^n, \quad V^Z = (\gamma_e S_z^e - \gamma_N S_z^n) B \quad (2)$$

for each of the atoms and two-body interaction terms V^c and V^d , representing the central interaction and the magnetic dipolar interaction, respectively. The central or exchange interaction represents an effective description of all Coulomb interactions between the electrons and nuclei and depends only on the magnitude of the total electron spin $\mathbf{S} = \mathbf{S}_1^e + \mathbf{S}_2^e$. It can be written as a sum of singlet and triplet terms:

$$V^c = V_0(r) P_0 + V_1(r) P_1, \quad (3)$$

with P_S projection operators on the subspaces with definite total electron-spin quantum number S . The dipolar interaction V^d is given by the familiar magnetic dipole-dipole expression. It is sufficient to include the electron-electron and electron-nuclear parts.

Asymptotically where the central and dipolar interactions can be neglected the system is described by the eigenstates of each of the atoms separately. In Fig. 1 the 16 (one-atom) ground-state hyperfine energies are shown

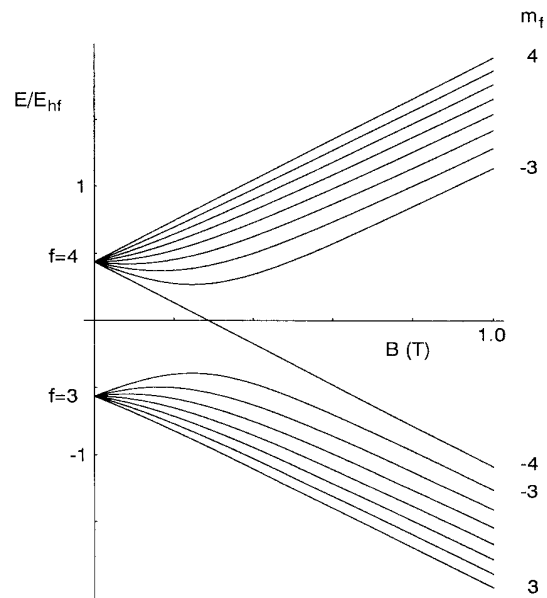


FIG. 1. Energies of ^{133}Cs hyperfine states, labeled fm_f , as a function of magnetic field. $E_{\text{hf}} = 4a_{\text{hf}}$ is the zero-field hyperfine splitting.

as a function of magnetic field. The one-atom hyperfine states are conveniently labeled with $|f, m_f\rangle$, where $\mathbf{f} = \mathbf{S}^e + \mathbf{S}^n$ is the total spin vector. Magnetic traps generally operate with fields well below the critical value $B_c = 4a_{\text{hf}}/(\gamma_e \hbar) \approx 0.33$ T, so that f is still a conserved quantum number. Figure 1 also shows that both $f=4$ and $f=3$ low-field-seeking states lend themselves to magnetic trapping. Since cesium atoms behave as bosons the wave function is required to be symmetric under exchange of atoms implying that for an even (odd) value of l the scattering channels have a symmetric (antisymmetric) spin structure. As a consequence, it is useful to introduce (anti)symmetrized two-body hyperfine states $|\{f_1 m_{f_1}, f_2 m_{f_2}\}^\pm\rangle$ for characterizing the scattering channels at infinity.

Independent of the nature of the interatomic interactions the projection of the total angular momentum $\mathbf{J} = \mathbf{L} + \mathbf{F}$ on the magnetic field axis z , with \mathbf{L} the relative orbital angular momentum of the atoms and $\mathbf{F} = \mathbf{f}_1 + \mathbf{f}_2$, the total spin, is conserved since an arbitrary rotation of the total system around this axis is a symmetry operation. For zero magnetic field J is a good quantum number as well.

Since V^c depends on r , it conserves the orbital angular quantum numbers l and m_l implying also that transitions between scattering states with different M_F are not allowed. To indicate the angular momentum structure of the dipolar interaction we express it in spherical tensor operators [18,19]:

$$V^d = -\frac{\mu_0 \mu_e^2}{4\pi r^3} \sum_{\mu=-2}^2 \left[\frac{4\pi}{5} \right]^{1/2} (-1)^\mu Y_{2,-\mu}(\hat{\mathbf{r}}) \Sigma_{2\mu}^{ee} + 2 \frac{\mu_0 \mu_e \mu_n}{4\pi r^3} \sum_{\mu=-2}^2 \left[\frac{4\pi}{5} \right]^{1/2} (-1)^\mu Y_{2,-\mu}(\hat{\mathbf{r}}) \Sigma_{2\mu}^{en}, \quad (4)$$

with $\Sigma_{2\mu}$ standing for a spin operator of rank 2. As a consequence it can change both the orbital angular momentum and the total spin quantum numbers, giving rise to so-called dipolar transitions satisfying $0 < |\Delta M_F| \leq 2$ and $|\Delta l| = 0, 2$ with $l=0 \rightarrow l=0$ forbidden. For the so-called exchange transitions with $\Delta M_F = 0$, which can be induced by the much stronger central interaction, the dipolar interaction has a negligible effect. From this it is clear that the (two-body) collisional decay of an arbitrary mixture of hyperfine states for Cs atoms in a magnetic trap takes place with two time scales [18,20]. On a short time scale all hyperfine states with $|m_f| < f$ disappear, since these can decay via exchange transitions. An interesting exception is the $|3, -2\rangle$ state for temperatures lower than $0.12[B(\text{T})]^2$ K, since then the $(3, -2) + (3, -2) \rightarrow (3, -3) + (3, -1)$ transition is energetically forbidden. The central interaction between two doubly-polarized $|4, +4\rangle$ atoms gives rise to purely elastic triplet scattering. Transitions to other channels and the associated decay of the density is therefore only induced on a longer time scale by the much weaker dipolar interaction. In a collision of two $|3, -3\rangle$ atoms the central interaction in principle allows transitions to other channels with $M_F = -6$ but as long as the collision ener-

gy is small relative to the hyperfine splitting $4a_{\text{hf}}$ such channels are closed. Dipolar transitions will again determine the lifetime of the gas.

A basis of spin states which is more fully adapted to the V^c and V^d terms is the set $|SM_S IM_I\rangle$ used extensively in previous hydrogen work [18], with \mathbf{I} the total nuclear spin. Keeping in mind that magnetic traps generally use magnetic fields well below B_c and the fact that both V^c and V^{hf} conserve \mathbf{F} , the basis $|(SIF)M_F\rangle$ sometimes offers advantages too. The atomic permutation symmetry of both types of basis states is characterized by $(-1)^{S+1}(-1)^{I+1}$ so that the above-mentioned Bose symmetry can be expressed by the requirement $l+S+I = \text{even}$.

In the latter basis it is illustrative to not only assume that B is small but also that a_{hf} is. The energy shifts to first order in a_{hf} can then be calculated by replacing V^{hf} by the equivalent expressions

$$\sum_i V_i^{\text{hf}} \rightarrow \frac{a_{\text{hf}}}{2\hbar^2} \mathbf{S} \cdot \mathbf{I} \rightarrow \frac{a_{\text{hf}}}{4} \{F(F+1) - S(S+1) - I(I+1)\}, \quad (5)$$

which is nonvanishing only for $S=1$. The hyperfine interaction is thus seen to lift the degeneracy of the triplet rovibrational bound states (and resonances) with respect to I and F . Both experiment [21] and our coupled-channel calculations for the discrete spectrum show that this first-order picture is valid for the lower part of the energy spectrum. For higher levels such as those corresponding to the scattering resonances showing up in the calculations of this paper a first-order picture is totally inadequate due to the fact that the energy distance of subsequent singlet and triplet vibrational states approaches the large value of the hyperfine constant a_{hf} for Cs. A particularly clear example of resonances showing these higher-order effects will be given in the following section (see the discussion of Fig. 4). Since the part of V^{hf} diagonal in S has already been covered completely by Eq. (5), the only part which is missing in the first-order picture is the mixing of singlet and triplet states of the same F . Owing to the Bose condition $l+S+I = \text{even}$, this mixing occurs only for $F < 8$ if $F = \text{even}$ (odd) for l even (odd).

Let us now turn to the influence of a nonvanishing but weak magnetic field. Since V^Z is a rank 1 term under rotations, the various F states will be coupled with the constraints $|\Delta F| = 0, 1$ and $\Delta M_F = 0$. Neglecting the much smaller nuclear Zeeman term, the energy splittings of the basis states $|(SIF)M_F\rangle$ due to the electronic Zeeman term can be calculated by replacing V^Z by the familiar equivalent Landé expression

$$\gamma_e S_z B \rightarrow \gamma_e B F_z \mathbf{S} \cdot \mathbf{F} / F^2 \rightarrow M_F \frac{\{S(S+1) + F(F+1) - I(I+1)\}}{2F(F+1)} \gamma_e \hbar B. \quad (6)$$

To understand the resonances seen in our coupled-channels results it will be necessary to take also the F

mixing due to higher-order V^Z terms into account.

Before actual calculations of transition probabilities and elastic cross sections can be made the singlet and triplet potentials are needed. To find them theoretically a many-electron problem would have to be solved which can only be done approximately. One can also use spectroscopic data on the rovibrational levels of the Cs_2 molecule. The same procedure as in Refs. [6] and [7] is used. For the singlet potential we use a spectroscopically determined Rydberg-Klein-Rees (RKR) potential from Weickenmeier *et al.* [22]. To obtain the triplet potential we reverse the exchange contribution of the singlet potential beyond $15.6a_0$, while for smaller internuclear distances we use an *ab initio* calculation by Krauss and Stevens [23] but modified in such a way that it fits with the position R_e of the minimum, the harmonic vibrational frequency ω_e , and the dissociation energy D_e given in Ref. [22]. There remains, however, a considerable uncertainty in the singlet and triplet potentials as indicated in Refs. [22] and [23]. It turns out from our calculations that the dipolar rates to be presented below are reliable to within an order of magnitude. Note in this connection that the dipolar rates in the case of atomic hydrogen can even be calculated reliably by leaving out the interatomic central potential altogether, i.e., by means of an excluded-volume plane-wave calculation [20]. A greater uncertainty is associated with a spin-spin term in the interatomic potential with presently unknown magnitude, which arises as a second-order effect in the electronic spin-orbit coupling [24,25] and therefore increases with Z . It has the same dependence on the atomic total electron spins as the dominant electron-electron part of the dipolar interaction, but it is a shorter-range interaction concentrated around the triplet minimum. It could increase the rate of “dipolar” decay of the $|4, -4\rangle$ state by an order of magnitude. Its role in the decay of the $|3, -3\rangle$ state is strongly reduced by the screening effect of the centrifugal barrier in each of the final channels (see Sec. V and Ref. [7]).

As already pointed out in Ref. [7], the present uncertainty in the central potential makes it impossible to predict the sign of the scattering length for $|4, 4\rangle + |4, 4\rangle$ elastic scattering, a crucial quantity for the realization of Bose-Einstein condensation in an atomic gas sample with only the $|4, 4\rangle$ hyperfine state occupied. The scattering length for the analogous $|3, -3\rangle$ elastic-scattering process can also be positive or negative, but in case of a negative sign the occurrence of resonances enables one to select a magnetic-field value at a resonance where the scattering length changes sign [7].

On the basis of the present knowledge of the triplet and singlet potentials it is impossible to predict the position and other properties of the resonances to be discussed below. The primary aim of this paper is rather to indicate the qualitative features expected to be observed experimentally. The measurement of the collisional frequency shift in the cesium fountain and of thermalization times and decay rates of cesium in a magnetic trap, and especially their resonance structure, will give information on how to improve the relevant properties of the potentials needed for more precise predictions.

At extremely large internuclear separations, of the order of the wavelengths ($\lambda \sim 2400a_0$) of optical transitions, the usual static electric multipole expansion is insufficient to describe the collisions and must be modified to incorporate retardation effects [26]. For such distances the central potentials fall off more rapidly, essentially like $1/r^7$ instead of the usual van der Waals $1/r^6$ behavior.

We rigorously solved coupled-channel equations distinguishing between three radial regions. Up to a radius $r_0 \approx 80a_0$ beyond which the exchange part of the central interaction, i.e., $V_1(r) - V_0(r)$, is negligible and the radial wave functions of the closed hyperfine channels are sufficiently small, we solved the differential equations in the SM_SIM_I basis. At this point the coupled equations were transformed to the hyperfine basis and integrated with the open hyperfine channels only from r_0 to a radius r_1 , where the central interaction itself becomes negligible. For larger distances the dipolar interaction is the only interaction taken into account and included in first order.

In view of the complicated spin structure due to the large value of the nuclear spin involved it is very difficult to do the associated Racah algebra by hand. We have used the computer algebra system MATHEMATICA to deal with this complicated task.

III. RESONANCES IN ELASTIC AND INELASTIC EXCHANGE SCATTERING

Figure 2 shows as an example the scattering length a for elastic scattering of two $|3, -3\rangle$ atoms as a function of magnetic field, calculated from the low-energy limit $-ka$ of the scattering phase shift. We see three resonances with very different strengths. The resonances also show up in the elastic scattering as a function of collision energy for fixed B . This enables us to follow them in a plane spanned by E and B . Figure 3 shows the paths obtained. Clearly, the resonance positions show an almost linear Zeeman-like behavior. The error bars denote the width of the second resonance which turns out to be almost constant in the E - B plane, while that of the two weaker resonances is very small and proportional to B^2

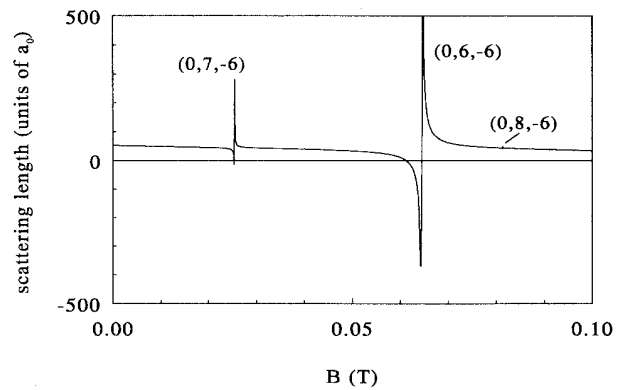


FIG. 2. Scattering length for elastic $|3, -3\rangle + |3, -3\rangle$ scattering as a function of magnetic field. Labels denote quantum numbers (l, F, M_F) .

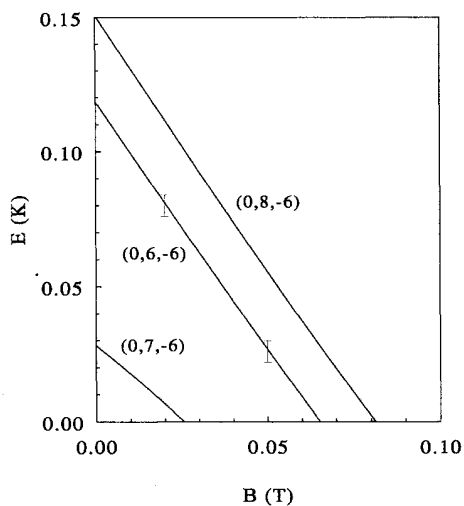


FIG. 3. Position and width of the $l=0$ and $M_F=-6$ resonances in the plane spanned by the collision energy of $|3,-3\rangle + |3,-3\rangle$ scattering and the applied magnetic field. Labeling is according to Fig. 2. The error bars of the $F=6$ resonance denote its width.

and B^4 for the first and third resonance, respectively.

Insight into the nature of these resonances can be obtained on the basis of the various existing more or less equivalent resonance theories formulated long ago for nuclear reactions [27]. In each of these theories resonances arise from the existence of discrete quasibound states. A resonance occurs in the scattering process due to the coupling of these quasibound states with the continuum of scattering states at infinity. The coupling is concentrated at collision energies close to the energy of a quasibound state and the overall strength of the coupling determines the partial and total resonance widths.

Figure 4 shows a systematic explanation for the positions of the resonances, introducing various interaction terms in the Hamiltonian one by one. We start with neglecting the hyperfine and Zeeman terms altogether. In that limit the quasibound states reduce to the bound $l=0$ rovibrational states of the singlet and triplet Cs_2 molecule with vanishing decay widths. In Fig. 4(a) the energies of these states are presented, together with the vibrational quantum number v . The energy scale is in degrees kelvin, the zero of energy corresponding to the threshold of the continuum of the singlet and triplet potentials. Figure 4(b) shows what happens to these states when the hyperfine term V^{hf} is gradually introduced, multiplying it by an auxiliary parameter λ varying from 0 to 1. The degeneracy of the original states with respect to I and F is then lifted, the spin states $|(SI)FM_F\rangle$ introduced in the preceding section being the appropriate basis. For small λ the levels split and shift according to the first-order perturbation result of Eq. (5). Since we restrict ourselves to the $M_F=-6$ resonances showing up in a $(3,-3)+(3,-3)$ collision, F is equal to 6, 7, or 8. Note that $S+I$ has to be even because of $l=0$. For larger values of λ pairs of bound states with equal F start to repel each other, giving rise to “avoided crossings.” The

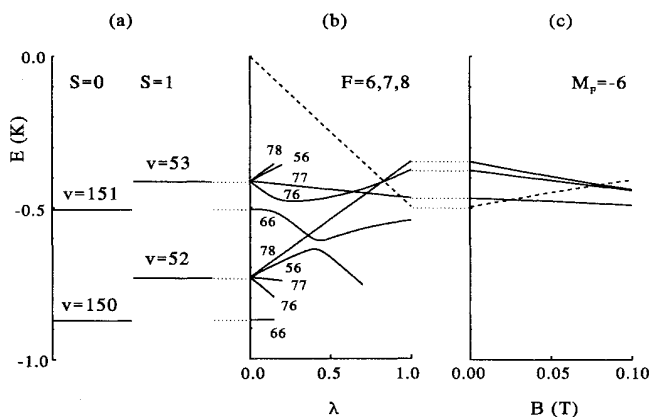


FIG. 4. Physical picture for $l=0$, $M_F=-6$ resonances. The vertical scale shows the total energy with zero energy located at the threshold of the continuum of the singlet and triplet potentials. (a) Energies of the relevant $l=0$ singlet and triplet bound states. (b) Resonance energies, labeled IF , splitted by hyperfine interaction. The dashed line is the hyperfine energy $-9\lambda a_{\text{hf}}/2$ of the $\{3-3,3-3\}^+$ state. (c) Resonance energies for $M_F=-6$ as a function of magnetic field. The dashed line is the hyperfine+Zeeman energy of the $\{3-3,3-3\}^+$ state.

repulsion can be understood in terms of the perturbations involving the coupling between the singlet $|(OF)FM_F\rangle$ and triplet $|(1,F\pm 1)FM_F\rangle$ levels, already dealt with in connection with Eq. (5). This coupling not only involves a spin-dependent factor, but also the radial overlap of the various singlet and triplet bound states. By symmetry $F=8$ and odd F triplet states do not couple, so that these states are described by Eq. (5) for all λ . This allows the possibility of an identification of the pure triplet resonances in our calculated cross sections. The dashed line in Fig. 4(b) shows the total hyperfine energy of two $|3,-3\rangle$ atoms. At the actual value of the hyperfine strength the positions of the $F=7$ and 8 states coincide with the two resonances in Fig. 3 which disappear at $B=0$. Since $|\{3-3,3-3\}^+\rangle$ is a pure $F=6$ state and different F values are only coupled by V^Z , this disappearance is not surprising. To find the exact positions of the $F=6$ bound states the coupling to all vibrational singlet/triplet states should be included. Neglecting the far levels a simple model with two triplet and one singlet vibrational level can be used to calculate the location of the broad $F=6$ resonance in Fig. 3. This model gives a level which lies within 5×10^{-3} K from the exact location. It should be noted that the mixing of v levels in the Cs_2 molecule is rather extreme, because the strong hyperfine splitting approaches the magnitude of the small vibrational energy distances.

Figure 4(c) finally shows how the $M_F=-6$ levels shift upon introducing a magnetic field. V^Z couples the subspaces with different F while conserving M_F . As long as this coupling is weak the energies of the magnetic substates, degenerate for $B=0$, split linearly with B . For $F=8$ and F odd the shift of the $M_F=-6$ levels depends solely on the spin structure as described by Eq. (6). For other F values the field dependence is given by the expect-

tation values of V^Z in the eigenstates obtained by the above-mentioned mixing of singlet and triplet levels. For stronger fields the off-diagonal part of V^Z becomes important. For $F=8$ or F odd these higher-order perturbations may even be included in a straightforward way, since one is dealing with pure $S=1$ states. In Fig. 4(c) the dashed line again gives the total (hyperfine + Zeeman) energy of the $|\{3-3,3-3\}^+\rangle$ state. The energy differences of the solid lines with this dashed line would have to agree with Fig. 3. For the $F=7$ and 8 resonances this indeed turns out to be the case. In particular, the intersection of the $F=7$ line, described with a linear model, with the dashed line reproduces the exact position of the corresponding resonance in the scattering length to within 5×10^{-4} T. For the $F=8$ line the error is ten times larger, showing that the linear approximation is slowly breaking down for the associated stronger field. The higher-order approach reduces the error to that for the linear $F=7$ line. The discrepancy for the $F=6$ resonance is much larger and given by 1×10^{-2} T, which is mainly due to the incorrect treatment of the strong hyperfine coupling. This discussion shows that the precise location of the resonances is directly related to the position of the unperturbed singlet and triplet vibrational levels around $E = -9a_{\text{hf}}/2$. The experimental observation of the resonances can be used to locate these bound states to within about 10^{-2} K. In Figs. 2 and 3 we have added the (l, F, M_F) quantum numbers for the resonances as they follow from the previous analysis.

In each of the above-mentioned resonance theories (see, for instance, Refs. [27,28]) the partial width of a resonance for decay into a particular scattering channel is proportional to $|\langle B | H_{\text{coup}} | \phi \rangle|^2$, where $|B\rangle$ is a quasi-bound state, $|\phi\rangle$ a scattering state, and H_{coup} the coupling between the two. Since in the present case the resonances can only be formed from and decay into the $|\{3-3,3-3\}^+\rangle$ channel, a partial resonance width is at the same time a total width. From the discussion of Fig. 4 it follows that the $F=6$ resonance has a width proportional to a_{hf}^2 , while for $F=7$ and 8 a magnetic field is essential for decay into an $F=6$ channel, so that the corresponding widths behave as B^2 and B^4 , respectively.

Ideally, it would have been illustrative if we could calculate both resonance energies E_R and widths Γ of the various resonances on the basis of one of the existing resonance theories. A particularly elegant framework would be the Rosenfeld-Humblet theory [29] which is based on the original idea of a Gamow decaying state, devised for α decay of atomic nuclei. The idea is to find solutions of Schrödinger's equation $H\Psi = E\Psi$ with "outgoing" waves in all channels at infinity. The associated complex eigenvalues $E_R - i\Gamma/2$ determine the resonance energies and widths. A practical implementation within a coupled-channels framework would involve an elaborate integration of a set of complex differential equations and a search in the complex energy plane for solutions with the correct asymptotic behavior. However, as long as the resonances are far apart the R -matrix approach [30] shows that their energies are well approximated using the Wigner-Eisenbud boundary condition $d\Psi/dr = b\Psi$ with a real constant b at a radius r_1 beyond which the central

interaction is negligible. Using this approach we indeed found the scattering resonances at the correct field values with positions rather insensitive to the value of b . In addition, however, we found spurious resonances introduced by the specific boundary condition, which we could distinguish from the real ones by their strong dependence on r_1 and b .

In the foregoing we restricted ourselves for simplicity to low-energy scattering in the $|\{3-3,3-3\}^+\rangle$ channel, because this involves exchange scattering with one open channel only. (In)elastic exchange scattering involving other open channels is more complicated but does not add fundamentally new aspects.

IV. RESONANCES IN DIPOLAR RATES

The dipolar transition rates turn out to contain resonances too. Since V^d is only important for the atom loss from the $|4, +4\rangle$ and the $|3, -3\rangle$ gas we restrict ourselves to these cases. The resonance structure is now complicated by the fact that the dipolar interaction is nondiagonal in l and M_F . Resonances thus show up not only in the lM_F subspaces of initial and final channels, but also in other subspaces coupled by additional V^d steps. Due to the weakness of V^d only resonances for which at most two V^d steps are necessary show up in our calculated results.

It turns out that resonances do not occur in the dipolar rates of the doubly polarized $|4, +4\rangle$ gas. This may be understood from the discussion of Fig. 4. Irrespective of the magnetic-field strength the total energy for a collision initiated in the $|\{44,44\}^+\rangle$ channel is located above the zero energy defined in this figure and therefore never crosses one of the bound rovibrational states. This is clear from Fig. 5, showing the zero-temperature dipolar

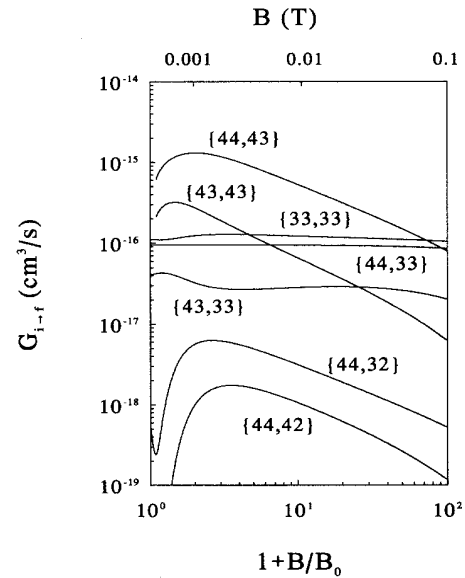


FIG. 5. $T=0$ dipolar relaxation rates $G_{i \rightarrow f}$ for the doubly polarized cesium gas as a function of magnetic field. Horizontally the quantity $1+B/B_0$ with $B_0 = a_{\text{hf}}/160\mu_B$ is plotted logarithmically. This ensures a favorable separation between linear and logarithmic parts.

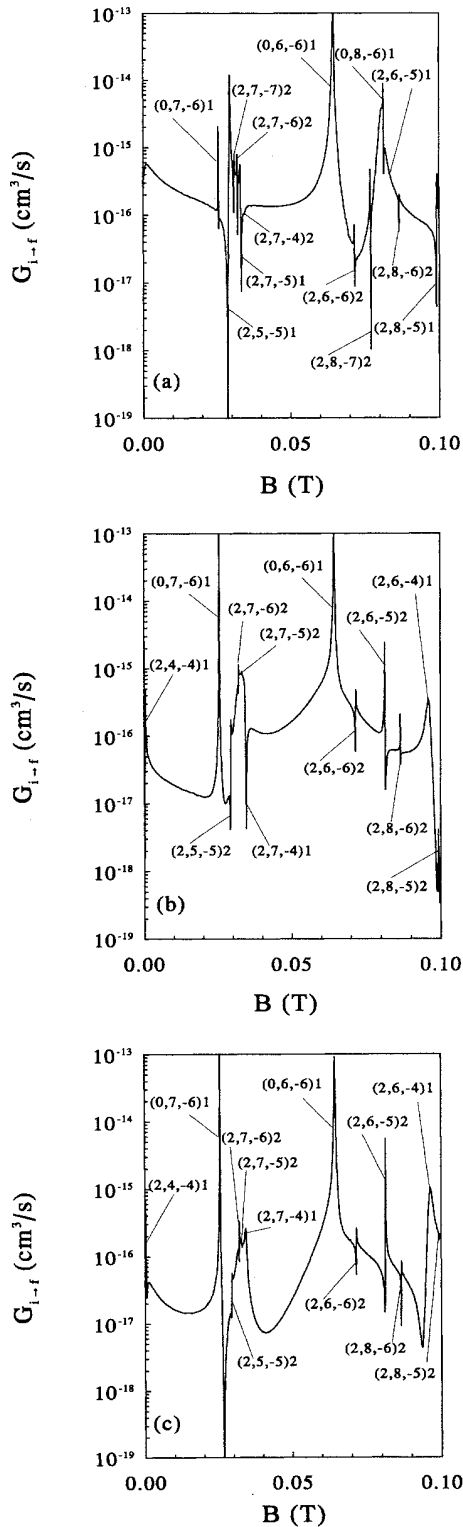


FIG. 6. (a) $T=0$ dipolar relaxation rates $G_{i \rightarrow f}$ for a gas of cesium atoms in the $|3, -3\rangle$ hyperfine state as a function of magnetic field. (a) Rate for $|3, -3\rangle + |3, -3\rangle \rightarrow |3, -3\rangle + |3, -2\rangle$. (b) Rate for $|3, -3\rangle + |3, -3\rangle \rightarrow |3, -3\rangle + |3, -1\rangle$. (c) Rate for $|3, -3\rangle + |3, -3\rangle \rightarrow |3, -2\rangle + |3, -2\rangle$. Labels denote (l, F, M_F, i) with i standing for the number of V^d steps for a resonance to contribute to the total transition amplitude considered.

decay rates for a doubly polarized $|4, +4\rangle$ gas as a function of B . The labels indicating the rates correspond with the notation $\{f_1 m_{f_1}, f_2 m_{f_2}\}$ for the final states.

In Fig. 6 the decay rates for a $|3, -3\rangle$ gas are shown. They do show a complex resonance structure. The three previously discussed $l=0, M_F=-6$ resonances are again present and in addition resonances of the subspaces with $l=2$ and $M_F=-4$ to -7 have appeared. The labels of each resonance give the corresponding l, F, M_F values. A detailed discussion of these additional resonances analogous to that in connection with Eq. (5) shows that those with $F=5, 7$, and 8 can be described in a simple way without singlet/triplet mixing. Only one triplet state is involved: $v=53$ for $F=5$ and 7 and $v=52$ for $F=8$. The states are shifted according to Eqs. (5) and (6) and in addition according to the rotational energy for $l=2$. The resonances with $F=4$ and 6 show a strong mixing of singlet and triplet bound states. In Fig. 6 we have also indicated the number of V^d steps needed for each of the resonances to contribute to the total transition amplitudes considered. The $l=0$ resonances associated with the subspace of the initial $M_F=-6$ channel and the $l=2$ resonances corresponding to the subspace of the final $M_F=-4$ or -5 channels clearly need only one V^d step. All other resonances need second-order V^d coupling.

V. INFLUENCE OF FINAL CENTRIFUGAL BARRIER

The influence of the centrifugal barrier in the final channel for a dipolar decay process is of utmost practical importance in that it may reduce the loss of atoms. Therefore we study it in some detail. For the low temperatures of experimental interest it suffices to consider $l=0 \rightarrow l=2$ transitions only. The role of the centrifugal barrier is immediately visible in the dipolar rates of the $|4, +4\rangle$ state to the $|\{44, 43\}^+\rangle$, $|\{44, 42\}^+\rangle$, and $|\{43, 43\}^+\rangle$ channels in Fig. 5, and in all three decay rates of the $|3, -3\rangle$ state in Fig. 6. They tend to zero as $B \rightarrow 0$, because the outer classical turning point in each of these final channels goes to $r = \infty$. We have been able to understand the more detailed B dependence and in particular its difference with the case of atomic hydrogen [18] by studying how the contributions to the total coupled-channel dipolar transition amplitudes are distributed over the r axis and making a comparison with that expected for a simple distorted-wave integral

$$\int_0^\infty u_f(r) \frac{1}{r^3} u_i(r) dr \quad (7)$$

with an initial $l=0$ triplet radial wave function at zero kinetic energy and a final $l=2$ radial wave function for a collision energy E_f proportional to $\mu_e B$. With the exception of the $|\{44, 44\}^+\rangle$ state, all spin states involved are actually combinations of $S=1$ and $S=0$ states. Since, however, only the triplet parts contribute to the dominating electron-electron term of the dipolar matrix element, the pure triplet case should give a semiquantitative picture. This is confirmed by introducing a radial cutoff for V^d in the full coupled-channel calculation and varying the cutoff radius.

The B dependence can be understood by considering

the competition of the contributions from a small- r and a large- r radial part of the integral (7), separated by the radius r_d . For lower fields where the final collision energy is below the top of the barrier, r_d is the outer turning point. For stronger fields where the final collision energy surmounts the barrier, r_d is the radius where the triplet interaction is equal to $6\hbar^2/2r^2 - E_f$ in absolute magnitude.

In the small- r part the triplet potential $\approx -c_6/r^6$ dominates in the radial equations so that the initial and final waves are proportional, contributing maximally to the radial integral. As a consequence, this contribution to the dipolar rate depends on the amplitude of the final wave function and on r_d . For weak magnetic fields the amplitude of this wave function is reduced starting from infinity due to the centrifugal barrier. For strong fields the WKB approximation becomes valid for all r . As a consequence, if we give the final wave function the usual WKB normalized amplitude $k_f^{-1/2}$ at infinity, the amplitude in the inner region is independent of B . Note that the chosen normalization corresponds exactly with the way in which $u_f(r)$ occurs in the dipolar rate expression. This would suggest that at strong fields the inner part of the dipole amplitude would tend to a constant, after an initial increase due to enhanced barrier penetration. However, r_d and thus the length of the inner region decrease, so that in total the amplitude decreases.

In the outer region the triplet potential is negligible. In general $u_f(r)$ oscillates much faster than $u_i(r)$, so that the integral is effectively limited to r values just outside the classical turning point of the final channel. This occurs for weak fields only. Increasing the magnetic field starting from zero enhances the dipole integral since the contributing region shifts to smaller r , so that the dipole interaction strength $\sim 1/r^3$ increases. However, increasing the magnetic field also shifts the oscillations of $u_f(r)$ to smaller distances from r_d , which counteracts the initial increase.

The relative importance of the inner and outer regions for reasonable values of B as considered in Figs. 5 and 6 is such that for $E_f > 10^{-3}$ K, or equivalently magnetic fields above $\approx 10^{-3}$ T, the inner region dominates. For lower fields the outer region dominates. This contrasts with calculations for atomic hydrogen [18], for which the contribution of the inner region is negligible even for

fields as high as 10 T. This is due to the high $l=2$ centrifugal barrier and the small c_6 . The hydrogen rates still show a “knee” shape for fields of about 0.1 T, but this is entirely due to the spin structure.

The remaining cesium dipole rates in Fig. 5 have a finite exothermal energy even for $B=0$. The large final collision energy E_f of order $a_{\text{hf}} \approx 0.1$ K leads to a dominating inner region contribution. The radius r_d is for large E_f approximately proportional to $E_f^{-1/6}$ and only slowly dependent on magnetic field. The dipolar rates are therefore only weakly dependent on B .

VI. CONCLUSIONS

On the basis of symmetry considerations with respect to the various interaction terms in the Hamiltonian, we have been able to give a detailed discussion of the resonances in the elastic and inelastic exchange scattering of two ultracold Cs atoms. Gradually switching on the hyperfine strength and the magnetic field, we were able to follow the resonance positions and widths in the E - B plane. In addition, the quantum numbers of the resonances could be identified. It was shown that the basis of $|(SI)FM_F\rangle$ states is particularly adequate for describing the physics of the resonances. A successful description could also be given for the more complicated resonance structure in the dipolar rates, distinguishing the numbers of V^d steps involved. It is expected that observation of the resonances will play a crucial role in determining the relevant parts of the triplet and singlet potentials which are presently insufficiently known.

The role of the $l=2$ centrifugal barrier in the final decay channel in determining the magnitude of the dipolar loss of atoms from a magnetic trap has been studied. The field dependence of the rates can be explained in terms of the competition between an inner and an outer radial region. Differences with atomic hydrogen have been pointed out.

ACKNOWLEDGMENT

This work is part of a research program of the Stichting voor Fundamenteel Onderzoek der Materie, which is financially supported by the Nederlandse Organisatie voor Wetenschappelijk Onderzoek.

-
- [1] J. Prodan, A. Migdal, W. D. Phillips, I. So, H. Metcalf, and J. Dalibard, *Phys. Rev. Lett.* **54**, 992 (1985); W. Ertmer, R. Blatt, J. L. Hall, and M. Zhu, *ibid.* **54**, 996 (1985).
 - [2] For a review we refer to the special issues of *J. Opt. Soc. Am. B* devoted to laser cooling and trapping: **2** (1985) and **6** (1989).
 - [3] M. Kasevich, E. Riis, S. Chu, and R. DeVoe, *Phys. Rev. Lett.* **63**, 612 (1989).
 - [4] A. Clairon, C. Salomon, S. Guellati, and W. D. Phillips, *Europhys. Lett.* **12**, 683 (1991).
 - [5] M. Kasevich, D. S. Weiss, and S. Chu, *Opt. Lett.* **15**, 607 (1990); H. Wallis, J. Dalibard, and C. Cohen-Tannoudji, *Appl. Phys. B* **54**, 407 (1992).
 - [6] E. Tiesinga, B. J. Verhaar, H. T. C. Stoof, and D. van Bragt, *Phys. Rev. A* **45**, R2671 (1992).
 - [7] E. Tiesinga, A. J. Moerdijk, B. J. Verhaar, and H. T. C. Stoof, *Phys. Rev. A* **46**, R1167 (1992).
 - [8] For a review we refer to the papers by T. J. Greytak and D. Kleppner, in *New Trends in Atomic Physics*, edited by C. Grynberg and R. Stora (North-Holland, Amsterdam, 1984), p. 1125, and to I. F. Silvera and J. T. M. Walraven, in *Progress in Low Temperature Physics*, edited by D. F. Brewer (North-Holland, Amsterdam, 1986), Vol. 10, p. 139.
 - [9] T. W. Hijmans, O. J. Luiten, I. D. Setija, and J. T. M. Walraven, *J. Opt. Soc. Am. B* **6**, 2235 (1989).

- [10] J. M. Doyle, J. C. Sandberg, I. A. Yu, C. L. Cesar, D. Kleppner, and T. J. Greytak, *Phys. Rev. Lett.* **67**, 603 (1991).
- [11] C. Wieman *et al.* (private communication).
- [12] J. J. Tollett, C. C. Bradley, and R. G. Hulet, *Bull. Am. Phys. Soc.* **37**, 1126 (1992).
- [13] T. Walker, D. Sesko, and C. Wieman, *Phys. Rev. Lett.* **64**, 408 (1990); D. Sesko, T. Walker, and C. Wieman, *J. Opt. Soc. Am. B* **8**, 946 (1991).
- [14] A. L. Fetter and J. D. Walecka, *Quantum Theory of Many-Particle Systems* (McGraw-Hill, New York, 1971), p. 222.
- [15] W. C. Stwalley, *Phys. Rev. Lett.* **37**, 1628 (1976); Y. H. Uang, R. F. Ferrante, and W. C. Stwalley, *J. Chem. Phys.* **74**, 6267 (1981).
- [16] M. W. Reynolds, I. Shinkoda, R. W. Cline, and W. N. Hardy, *Phys. Rev. B* **34**, 4912 (1986).
- [17] I. F. Silvera, H. P. Godfried, E. R. Eliel, J. G. Brisson, J. D. Gillaspay, J. C. Mester, and C. Mallardeau, *Phys. Rev. B* **37**, 1520 (1988).
- [18] H. T. C. Stoof, J. M. V. A. Koelman, and B. J. Verhaar, *Phys. Rev. B* **38**, 4688 (1988).
- [19] A. Messiah, *Quantum Mechanics* (North-Holland, Amsterdam, 1965).
- [20] A. Lagendijk, I. F. Silvera, and B. J. Verhaar, *Phys. Rev. B* **33**, 626 (1986).
- [21] H. Weickenmeier, U. Diemer, W. Demtröder, and M. Broyer, *Chem. Phys. Lett.* **124**, 470 (1992).
- [22] H. Weickenmeier, U. Diemer, M. Wahl, M. Raab, W. Demtröder, and W. Müller, *J. Chem. Phys.* **82**, 5354 (1985).
- [23] M. Krauss and W. J. Stevens, *J. Chem. Phys.* **93**, 4236 (1990).
- [24] P. S. Julienne, F. Mies, and C. Williams (private communication).
- [25] S. R. Langhoff, *J. Chem. Phys.* **61**, 1708 (1974); P. S. Julienne, *J. Mol. Spectrosc.* **56**, 270 (1975).
- [26] W. J. Meath and J. O. Hirschfelder, *J. Chem. Phys.* **44**, 3210 (1966).
- [27] R. Huby, in *Nuclear Structure*, edited by A. Hossain, H. A. Rashid, and M. Islam (North-Holland, Amsterdam, 1967), p. 11.
- [28] H. Feshbach, *Ann. Phys.* **5**, 357 (1958).
- [29] J. Humblet and L. Rosenfeld, *Nucl. Phys.* **26**, 529 (1961).
- [30] E. G. Wigner and L. Eisenbud, *Phys. Rev.* **72**, 29 (1947); A. M. Lane and R. G. Thomas, *Rev. Mod. Phys.* **30**, 257 (1958).